Atmósfera 19(4), 213-234 (2006)

Diagnostic of cyclogenesis using potential vorticity

H. A. BASSET and A. M. ALI

Department of Astronomy and Meteorology, Faculty of Science,
Al-Azhar University, Cairo, Egypt.
Corresponding author: H. Basset; e-mail: hesmatm@yahoo.com

Received September 5, 2005; accepted February 12, 2006

RESUMEN

En las latitudes medias los ciclones y los anticiclones son los sistemas meteorológicos dominantes a escala sinóptica. Una manera atractiva de estudiar los aspectos dinámicos de estas estructuras es utilizar el marco de la vorticidad potencial (PV). En este trabajo se investigan varios aspectos de la ciclogénesis de latitudes medias utilizando los análisis de un caso de estudio dentro de este marco. El análisis de la vorticidad asoluta, relativa y potencial implica la significancia de la dinámica de los niveles altos en la iniciación de este caso de ciclogénesis. Por un lado, el análisis de la vorticidad isobárica parece ser informativo, exacto y fácil de utilizar como método para describir la dinámica de los niveles altos. Por otro lado, el análisis de la PV proporciona una imagen resumida del desarrollo y la evolución en los niveles altos y bajos, lo que es directamente visible, con base en un número pequeño de gráficas comparado con el del análisis de la vorticidad isobárica. El despliegue de la secuencia de tiempo de la PV en la superficie isentrópica apropiada ayuda a entender fácilmente la dinámica tridimensional del desarrollo del nivel alto.

ABSTRACT

Cyclones and anticyclones are the dominant synoptic scale meteorological systems in midlatitudes. An attractive way to study dynamical aspects of these structures is provided by the use of potential vorticity (PV) framework. In this paper several aspects of midlatitude cyclogenesis are investigated within this PV framework using a case study analysis. The analysis of absolute, relative and potential vorticity implies the significance of the upper level dynamics in the initiation of this case of cyclogenesis. On one hand, the isobaric vorticity analysis appears to be informative, accurate and easy to use as a method for describing the upper-level dynamics. On the other hand the PV analysis provided a summarized picture of the development and the evolution at upper and lower levels, which is directly visible, on the basis of a smaller number of plots compared with the isobaric vorticity analysis. The display of the time sequence of the PV on the appropriate isentropic surface helped in easily understanding the dynamics of the three-dimensional upper level development.

Keywords: Cyclogenesis, potential vorticity, vorticity analysis, isentropic, Mediterranean.

1. Introduction

In recent years, cyclogenesis over the central Mediterranean region has become the subject of considerable research (Prezerakos, 1991, 1992; Prezerakos *et al*., 1999; Karacostas and Flocas, 1983; Flocas and Karacostas, 1996), since these synoptic-scale events cause intense winds, precipitation and temperature drop. Because of the intimate connection between the phenomena and local weather prediction, interest in understanding the characteristics of cyclogenesis over this region is enormous and ongoing.

On the other hand, in the last decade, great emphasis has been placed on the analysis of the isentropic potential vorticity. Although, this dynamic atmospheric parameter was introduced in the 1940s by Rossby (1940) and Ertel (1942), its application in meteorological research was limited, mainly because of the complexity of its calculation. Since Hoskins *et al.* (1985) acknowledged the analysis of isentropic potential vorticity as a very important diagnostic tool to understand the mechanisms responsible for atmospheric development, the interest of the research community has increased enormously in this topic.

According to Hoskins *et al*. (1985), the potential vorticity analysis on isentropic surface summarizes the combined effect of the vorticity and temperature advection and allows the estimation of the vertical motion. The objective of the present work is to diagnose our case of study in the context of absolute, relative and potential vorticity analysis in order to examine in detail the key dynamical aspects of the cyclonic development.

2. Data and methodology

The data used in this study were obtained from the archives of the European Center for Medium-Range Weather Forecasts (ECMWF). They consist of the horizontal wind components (*u*-eastward, *v*-northward), the temperature (*T*), the relative humidity (*RH*) and the geopotential height (z) on regular latitude-longitude grid points resolution of $2.5° \times 2.5°$ for the isobaric levels 1000, 850, 700, 500, 300, 200 and 100 hPa. The data used are only at 1200 GMT during the period from 18 to 25 January 1981 (the life cycle of our cyclone). The domain of study extends from 15° W to 50° E and from 15° N to 60° N.

The inner domain which is used for the present study changes with time to enclose the cyclone during its life cycle. The computational inner domain extends from 15° W to 25° E and from 30° N to 60° N on 18 and 19 January and from 0° E to 40° E and from 25° N to 55° N on the following days. Centered finite differences were used to compute horizontal derivatives and all vertical derivatives except those at the 1000 and 100 hPa, where non-centered differences were employed. The vertical motion, *w*, is computed using the Q-vector representation of the quasi-geostrophic w equation by using the relaxation method (Krishnamurti and Bounoua, 1996). The relative vorticity and absolute vorticity advection have been calculated from the actual data using the central finite differences method.

It is well known (Petterssen, 1956; Palmen and Newton, 1969; Carlson, 1991) that the isobaric absolute vorticity together with their respective advections, are effective diagnostic tools for studying

the development of synoptic-scale extratropical atmospheric circulation systems. The local rate of change of relative vorticity is derived from the simplified vorticity equation (Holton, 1979; Wiin-Nielsen 1973; Carlson, 1991):

$$\frac{\partial \zeta}{\partial t} = -V.\nabla_p (\zeta + f) - f_0 \nabla_p .V \quad (1)$$

Where, **V** is the horizontal wind velocity, $f = f_0 + df / dy$ is the Coriolis parameter, with f_0 being the Coriolis parameter at reference latitude φ_0 and y the longitudinal distance, ∇ is the horizontal gradient operator applied with pressure held constant, $\zeta = k.\nabla \times \mathbf{V}$ is the vertical component of relative vorticity. In equation (2.1), the first right-hand term is the horizontal advection of absolute vorticity and the second is the divergence term. This equation could be replaced by the quasi-geostrophic vorticity equation. The increase in relative vorticity near the surface depends mainly on the convergence term (development term), in the middle troposphere on the advection term, since convergence is almost zero (level of non divergence), while near the tropopause both terms are significant.

2.1 Estimation of potential vorticity

A principal indicator of a fold like ingress of stratospheric air into the troposphere is the occurrence of an anomalous high potential vorticity value reaching down towards middle tropoppheric height levels. Hence, potential vorticity fields were calculated from the available meteorological parameters, namely temperature and the horizontal wind components on constant pressure surface. In isobaric coordinates the potential vorticity was approximated by the product of the vertical components of absolute vorticity and potential temperature gradients as

$$(PV)_\theta = \left[\left(\frac{\partial v}{\partial x} - \frac{\partial u}{\partial y} \right) + f + \frac{R}{\sigma P} \left(\frac{\partial v}{\partial p} \frac{\partial T}{\partial x} - \frac{\partial u}{\partial p} \frac{\partial T}{\partial y} \right) \right]_p \frac{\partial \theta}{\partial p} \quad (2)$$

where f is the coriolis parameter, q is the potential temperature u the wind in x-direction of the grid (W-E in principle) and v the wind in y-direction.

Following WMO (1986) the dynamic tropopause is defined by the potential vorticity with P= 1.6 x 10^{-7} Kpa^{-1} s^{-1} = 1.6 PVU, where, for convenience, the potential vorticity unit (PVU) is defined to be x 10^{-7} Kpa^{-1} s^{-1}.

3. Synoptic discussion

This cyclone evolves between 1200 GMT 18- 25 January 1981, while a strong cyclogenesis occurred during 1200 GMT 20-22 January 1981 over the Mediterranean Sea. Figs. 1 and 2 show the 1000 hPa and 500 hPa geopotential analysis for the period from 18 to 25 January respectively. Based on 1000

hPa charts, changes in the central of the low, and charts of 500 hPa the life cycle of the cyclone can be divided as follows: the first two days (18-19 January) immediately precedes the onset of cyclogenesis and can be termed as the precyclogenetic period. The third, forth and fifth days (20, 21 and 22 January) are the growth period, and finally the last three days (23, 24 and 25 January) are the decay period. At 1200 GMT 19 January, figures 1b and 2b show that a weak cyclonic system with surface center of 60 geopotential meter (gpm) is located over Greece and is associated with a baroclinic upper air trough. During the next 24 h, the center of the low propagates slowly northeastward, joins with the northwest cyclone and deepens to 40 gpm (Fig. 1c). A corresponding cut-off low formed at 500 hPa on 20 January over Italy with center of 5280 gpm. On 21 January, figures 1d and 2d show that the low pressure was deepened to −100 gpm and moved southeast to a point just south of Greek mainland. The development of the upper air trough was accompanied by cyclogenesis that started on 20 January, associated with a cut-off low formed at 500 hPa over Germany and Hungary at the eastern flank of an unstable large scale ridge with center of 5340 gpm. Meanwhile, the Siberian high extended to include most of the northeast of Europe while an extension of Azores anticyclone appeared as a new high-pressure center developed over the north of France. On 22 January, figure 1e indicates a southeast movement of the cyclone with slight filling to become −60 gpm at 1000 hPa, while the high pressure area intensified to include most of north Europe as shown from the 1000 hPa analysis. During the following two days (23 and 24 January) the depression started filling and its central pressure increased gradually. On the other hand the high pressure over the Atlantic extended further to form a major closed cell on 22 January (Fig. 1e) consequently no more cold advection was permitted to the cyclone. While the Azores high pressure extended eastwards, the horizontal extension of the cyclone decreased and moved slowly eastward, and became a stationary vortex rotating above the northeast of the Mediterranean. Finally, the cyclone drifted slowly northeastward and was out of the computational domain after 25 January.

4. Isobaric vorticity analysis

It has been recognized that central Mediterranean and northern African cyclogenesis is usually forced by a variety of upper-level tropospheric features, while the lower tropospheric physical and dynamic processes follow baroclinic instability (Karein, 1979; Prezerakos, 1992; Prezerakos *et. al*., 1992). This is associated with the theory of Helmholtz (Petterssen, 1956) that supports the controlling of the relation between the low level baroclinity and the surface cyclogenesis by the upper level forcing. The upper air circulation features originating in northwest Europe that have been recognized as precursors of central and eastern Mediterranean cyclogenesis (Prezerakos, 1992) are as follow: a) Strong and rapid cold advection towards the central Mediterranean in the upper troposphere, associated with the mobile jet streaks appearing upon the flanks of an omega shaped blocking anticyclone centered on the British Isles, b) The formation of a dynamically unstable ridge on the eastern flank of the above mentioned blocking high, c) The evolution of an upper diffluent trough, due to the asymmetrical flow between its western and eastern sides, and d) The upper tropospheric cold dome in connection with its contribution to surface cyclogenesis. Therefore, the identification and investigation of the upper tropospheric features that led to surface cyclogenesis on 20, 21 and 22 January is of major importance for forecasting the event.

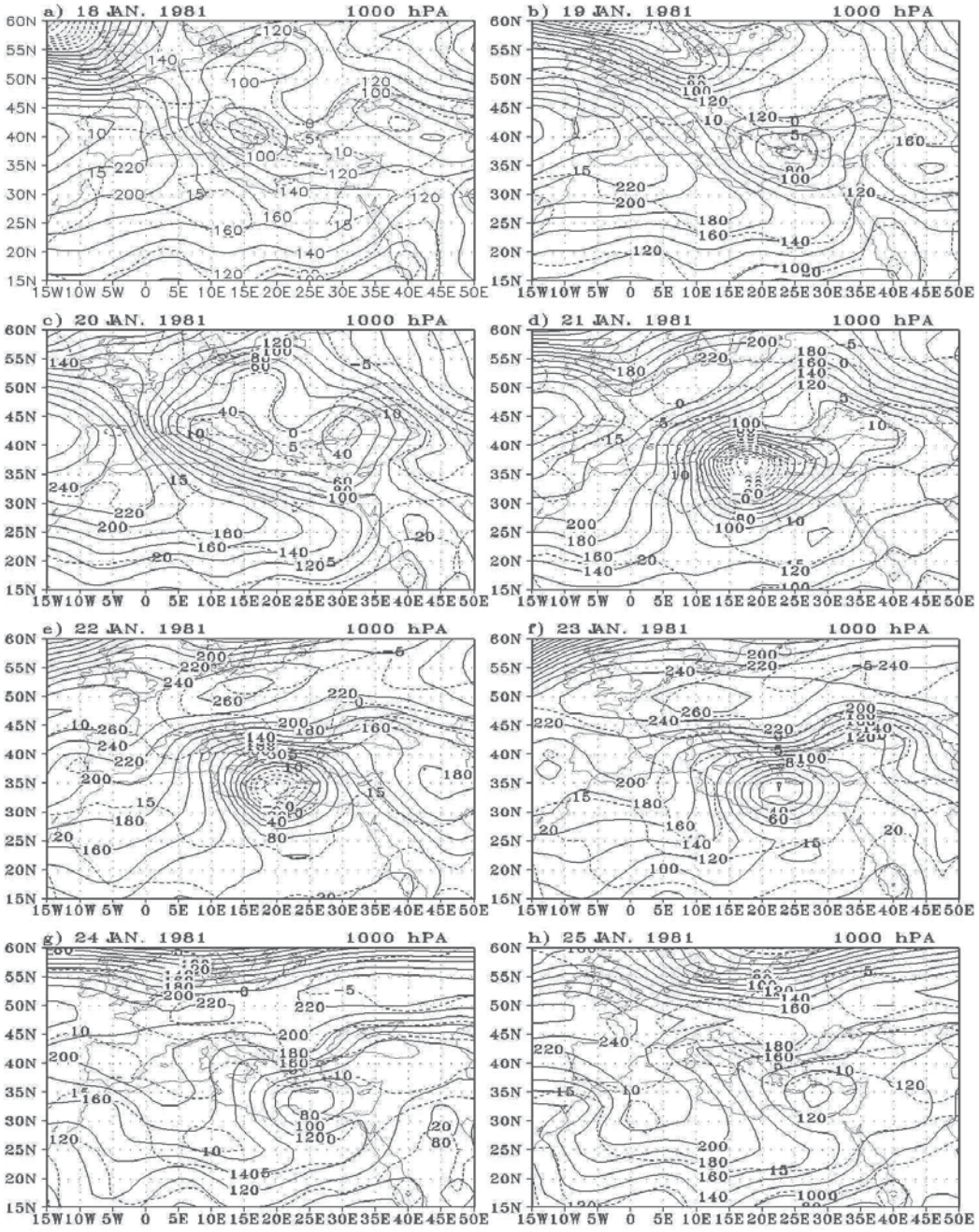

Fig. 1. The 1000 hPa geopotential contour every 20 m intervals (solid) and temperature dashed every 5 °C for 1200 UTC 18-25 January 1981.

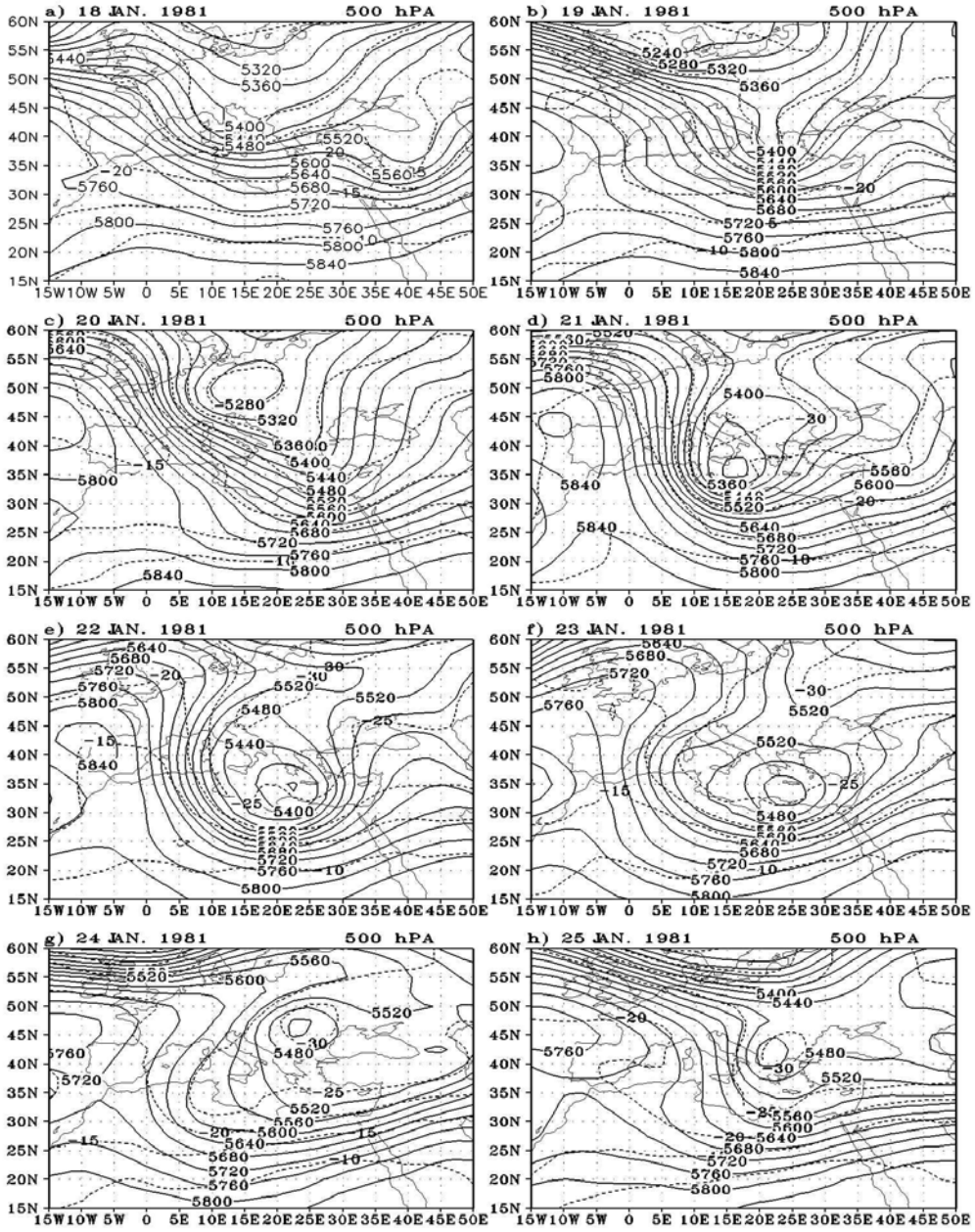

Fig. 2. The 5000 hPa geopotential contours every 40 m intervals (solid) and isotherms (dashed) every 5 °C for 1200 UTC 18-25 January 1981.

4.1 Genesis of the initial disturbance at the upper levels

It is known that the subtropical jet has its maximum speed around 200 hPa and the polar jet around 300 hPa. So, we display the 300 and 200 hPa isotach fields in the following discussion to show the behavior of the polar and subtropical jets during the development of this case study. Figures 3 and 4 display the isotachs at 300 and 200 hPa from 18 to 25 January 1981. They show the behavior of the subtropical and polar jets at 200 and 300 hPa levels during the life cycle of the cyclone.

At 18/12 an omega-shaped blocking over Northeast Atlantic and western Europe dominated the large-scale upper tropospheric circulation with a strong northwest-southeast jet stream on its eastern flank (Fig. 5). Because of the warm advection in the region of the jet streak, the ridge propagated slowly north-eastwards, resulting in the amplification of the long wave. On 19 January (Fig. 4b) the wind direction over North Africa was almost zonal and the maximum speed of the subtropical jet was 65 m/s located northeast of Africa (over Libya, Egypt and north Red sea), its value at 200 hPa was greater than 65 m/s. The polar jet extended from northwest England to southeast Spain and north of Italy with a maximum wind greater than 70 m/s at 300 hPa, its extension at 200 hPa had a maximum wind greater than 60 m/s.

As the polar jet streak moved south-eastward the cold air was advected continuously southward, consequently in the following 24 h (Fig. 5c), the baroclinity ahead of the ridge increased. The synoptic situation at 300 hPa on the following two days (Figs. 5c and 5d) was particularly important for the subsequent development. On 20 January, the subtropical jet moved slightly northeastward and its maximum center became greater than 60 m/s at 300 and 200 hPa and was located over Egypt. While the polar jet moved southeastward to amalgamate with the subtropical jet its maximum value became greater than 70 m/s at 300 and 200 hPa. On this day (20 January) the system becames cut off at all the isobaric levels, associated with relative vorticity maximum of $1.0 \times 1.0^{-4} s^{-1}$ at 500 hPa (Fig. 6c) and $1.4 \times 10^{-4} s^{-1}$ at 300 hPa (not shown), and increased baroclinity at these levels. At the surface, a frontal surface low becomes very pronounced and located over Italy parallel to the head of the polar jet stream. Therefore, when this type of atmospheric circulation dominates at the upper levels, intense surface cyclogenesis over the central Mediterranean is likely to be initiated, of course under favourable low level conditions (Prezerakos, 1992).

On 21 January, the subtropical jet shifted to the southeast. The front of the polar jet reached north of Algeria and its jet maximum wind value was greater than 70 m/s at 300 and 200 hPa. The subtropical jet weakened at 300 hPa and became stronger at 200 hPa (>70 m/s) and moved eastward. This day (21) represents the maximum amalgamation between the two jets. Beginning with the day 22 up to 24 January the polar jet became very weak at 300 hPa and its extension on 200 hPa disappeared. Also, we noticed that the subtropical jet moved eastward and were almost back to the normal distribution in both, speed and direction.

4.2. Initiation of the surface cyclogenesis

Figure 6 shows the relative vorticity at 500 hPa during the period of interest. Attention is focused on the center of maximum relative vorticity ($6.0 \times 10^{-4} s^{-1}$) found in the northwestern of the domain (Fig. 6a).

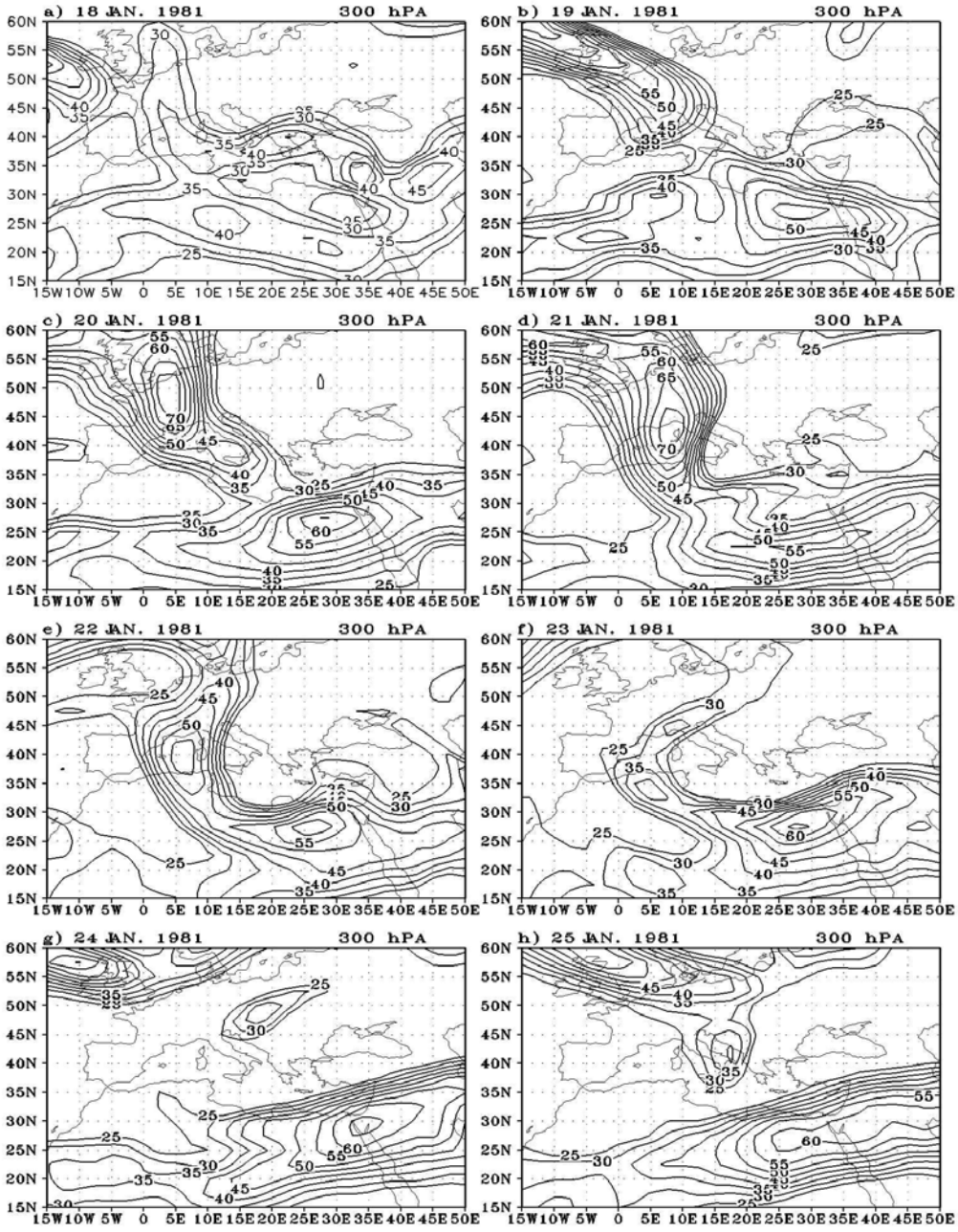

Fig. 3. Isotachs at 300 hPa, those ≥ 25 m/s, every 5 m/s,
for 1200 UTC 18-25 January 1981.

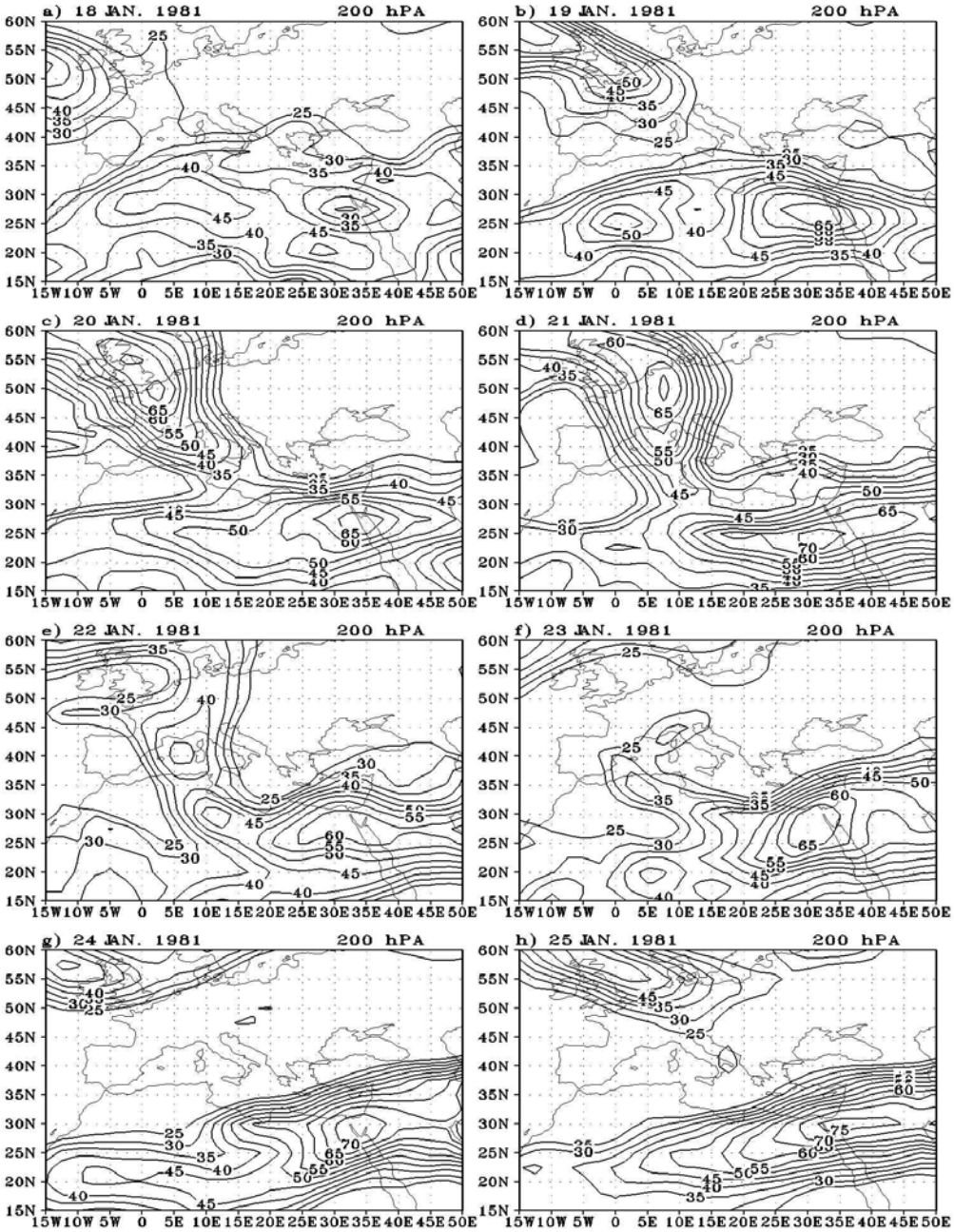

Fig. 4. Isotachs at 200 hPa those ≥ 25 m/s, every 5 m/s,
for 1200 UTC 18-25 January 1981.

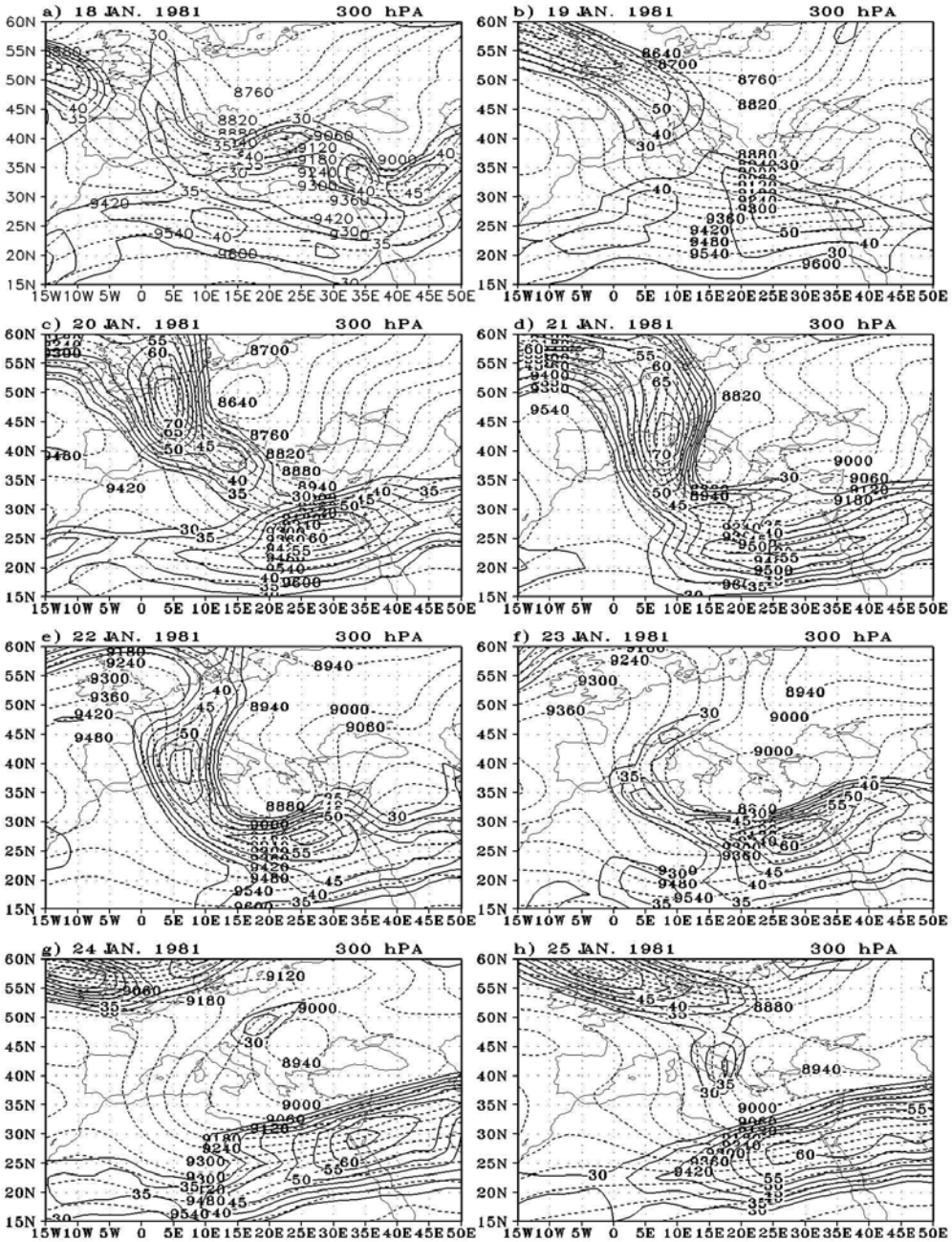

Fig. 5. 300 hPa geopotential contours every 60 gpm intervals dashed and isotachs solid those ≥ 30 m/s every for 1200 UTC 18-25 January 1981.

After 24 hours this center was strengthen and moved southeastward, its value reached $1.0 \times 10^{-4} s^{-1}$. On 20 January the center moved southwestward and originated at 47.5° N, 7.5° E, while another cell was found over north Egypt. By 21 January the maximum relative vorticity, located at 47.5° N, 7.5° E, moved westwards with a value of $1.2 \times 10^{-4} s^{-1}$ over 35° N, 15° E. Figure 6e shows that the cell of positive relative vorticity occupied a large area of the domain while its maximum decreased to $1.0 \times 10^{-4} s^{-1}$. Starting from 23 January the values of positive vorticity decreased gradually to reach its smallest area and lowest values on 25 January.

Figure 7 shows the field of relative vorticity at 850 hPa during the period of study. It shows that the relative vorticity undergoes a rapid change of magnitude, orientation and horizontal extension from day to day. At 18/12 we have three cells of maximum relative vorticity, the first is located at (57° N, 12.5° W) while the other two cells are at 40° N, 15° E and 55° N, 22° E. Here we are concerned with the first cell, which represents and accompanies the cyclone development. During the next 24 hours (the first cell) moved southeastward and its center was located at 52.5° N, 10° E, while the other two cells moved eastwards. By 20/12 the first cell divided into two other cells, the largest one moved southwestward 42° N, 5° E while the other originated at 52° N, 15° E. The maximum value of the relative vorticity of the second cell is $5 \times 10^{-5} s^{-1}$, while it is greater than $7 \times 10^{-5} s^{-1}$ for the first cell (Fig. 7c). During the next 24 hours the first cell underwent a rapid change in its position and magnitude, its center moved about 10 latitude degrees southeastward and its magnitude increased to $1.4 \times 10^{-4} s^{-1}$ at 37.5° N, 17.5° E. On the following 24 hours, this center moved rather slowly southeastward and its value decreased to $1.2 \times 10^{-4} s^{-1}$. In the last three days the values of the center of relative vorticity decreased gradually to reach its minimum on 25 January.

Figure 2c shows that a synoptic-scale wave is present over northwestern Europe at the isobaric ¿ ? level of 500 hPa and **its trough gets, with a** northeast-southwest tilt. The jet wind maximum is 70 m/s at 300 hPa (Fig. 3c). The wind speed decreased along the jet stream axis from west to east side of the trough resulting in an increase of the mean absolute vorticity advection in its region. Indeed, the left side region of the jet stream axis (polar jet) is characterized by positive advection of absolute vorticity with a maximum of $3.5 \times 10^{-9} s^{-2}$ shown as a filled circle in Figure 6, which was moving rapidly southwards. According to Petterssen (1956) and Kurz (1994), this synoptic situation is a precursor to cyclonic development. In association with the absolute vorticity advection, Austria and northern Italy were covered by a field of ascending motion at the isobaric level of 500 hPa, with the strongest ascent of 0.8 Pa s^{-1} laying over northern Italy. The positive relative vorticity had increased to $1.2 \times 10^{-4} s^{-1}$ over the central Mediterranean by 21 January, while the whole of Italy was characterized by positive absolute vorticity advection, implying the deepening of the upper trough.

The maximum absolute vorticity advection, located at 32.5° N, 15° E had intensified to $4.0 \times 10^{-9} s^{-2}$, where the ascending motion become as high as 1 Pa s^{-1} at 500 hPa (Fig. 8d). The relative humidity at 850 hPa was more than 90 % as shown in Figure 9d. According to the 1000 hPa analysis (Fig. 1d), the low-pressure center had developed over that area by 21/12, as the frontal zone had moved to the same region being under the maximum absolute vorticity advection (Fig. 6d). It is noteworthy that at the time of the surface cyclogenesis over central and eastern

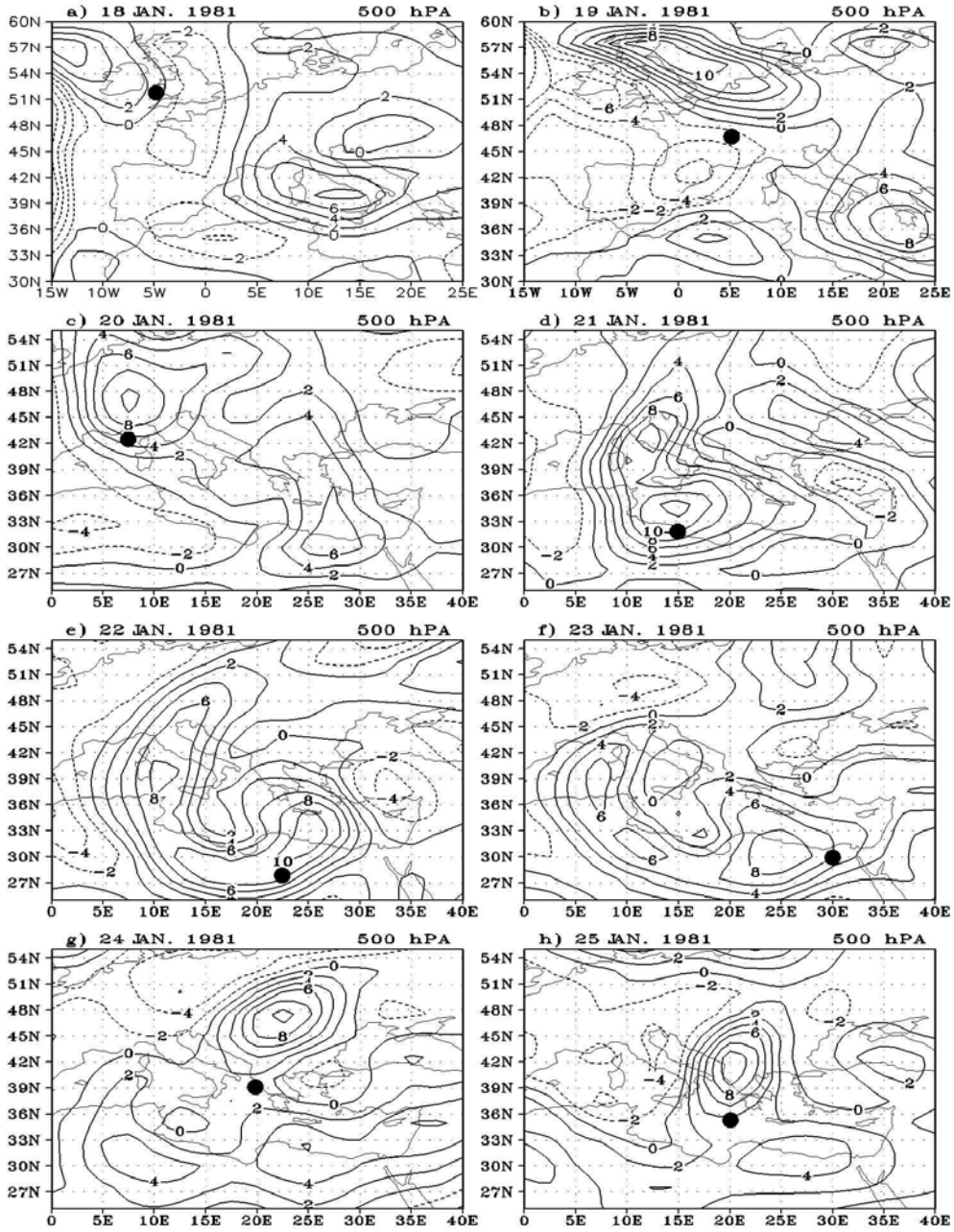

Fig. 6. Relative vorticity analysis at 500 hPa, contours every $2.0 \times 10^{-4}\ S^{-1}$, solid lines denote positive values, dashed lines denote negative values. Also indicated are the centers of 500 hPa maximum absolute vorticity advection (filled circle) for 1200 UTC 18-25 January 1981.

Mediterranean had intensified, the 300 hPa isotach analysis (Fig. 3d) suggests that the northerly polar frontal jet, curved cyclonically over central Mediterranean, tended to interact with the westerly subtropical jet that had propagated along the Libyan coast. By 21/12 as the orientation of the trough axis at 500 hPa had changed from northeast-southwest to north-south, extensive cyclonic development was marked (Carlson, 1991) and the low center at 500 hPa tended to develop (Fig. 2d). The surface low-pressure system became circularly organized and it deepened significantly near longitude 20° E. Figure 1d exhibits a significant westward tilt with height, indicating a strong baroclinic atmospheric environment. The maximum value of relative vorticity is in excess of $1.2 \times 10^{-4}\,s^{-1}$ (Fig. 6d), while the absolute vorticity advection is maximized in the vicinity of the surface cyclone system, reaching $4.0 \times 10^{-9}\,s^{-2}$. The ascent pattern had drifted eastwards over the same region, peaking at 1 Pa s^{-1} at 500 hPa (Fig. 8d) ahead of the surface system. A major factor allowing the surface low to convert available potential to kinetic energy is the advection of sinking cold air behind, and the advection of ascending warm air ahead of the low. This is especially evident at the 500 hPa isobaric level, in association with the vertical velocities chart (Fig. 8d).

In the following 24 hours, the depression moved rather slowly, following the absolute vorticity advection maximum (Fig. 6e). As seen in Figure 1d maximum development occurred at 21/12, when the surface system was situated between South of Italy and Greece. The central pressure had dropped 20 hPa in 24 hours (not shown). Nevertheless, the closed system does not seem to satisfy the appropriate critical pressure rate in order to be classified as a bomb, according to Sanders and Gyakum (1980). By this time the maxima of vorticity and vorticity advection had weakened substantially (Fig. 6e), that is the weakening of relative vorticity and absolute vorticity advection at 500 hPa had started before the surface pressure adopted its lowest value.

At this stage the system became cut off at all the isobaric levels. It is noteworthy that the system starts cut off at 500 hPa at 22/12, 24 h after cyclogenesis had commenced. Its vertical tilt with height implies that it continued growing almost barotropically.

5. Potential vorticity analysis

In order to highlight the dynamical significance of the most important features that the synoptic overview and the relative vorticity analysis revealed, and to identify other distinct characteristics of the development, a PV analysis is carried out. In particular, the distributions of isentropic PV along with that of the potential temperature at the tropopause have been used to examine the upper level development. The low-level evolution has been investigated in terms of isobaric distribution of PV.

5.1 Upper level development

Figure 10 summarizes the evolution of the PV field on the 320 °K isentropic surface from 18 to 25 January. Figure 10a displays three distinct anomalies: i) one of magnitude 4 PVU located northwest of England which represents and accompanies the cyclone of our interest, ii) one of magnitude 4 PVU that appeared over Italy and iii) one over northern Europe (60° N, 10° E). According to Figure 10b, within 24 hours the first PV maximum (which is of our interest) propagated slightly southeastwards and its magnitude reached to 6 PVU while the second and the third propagated

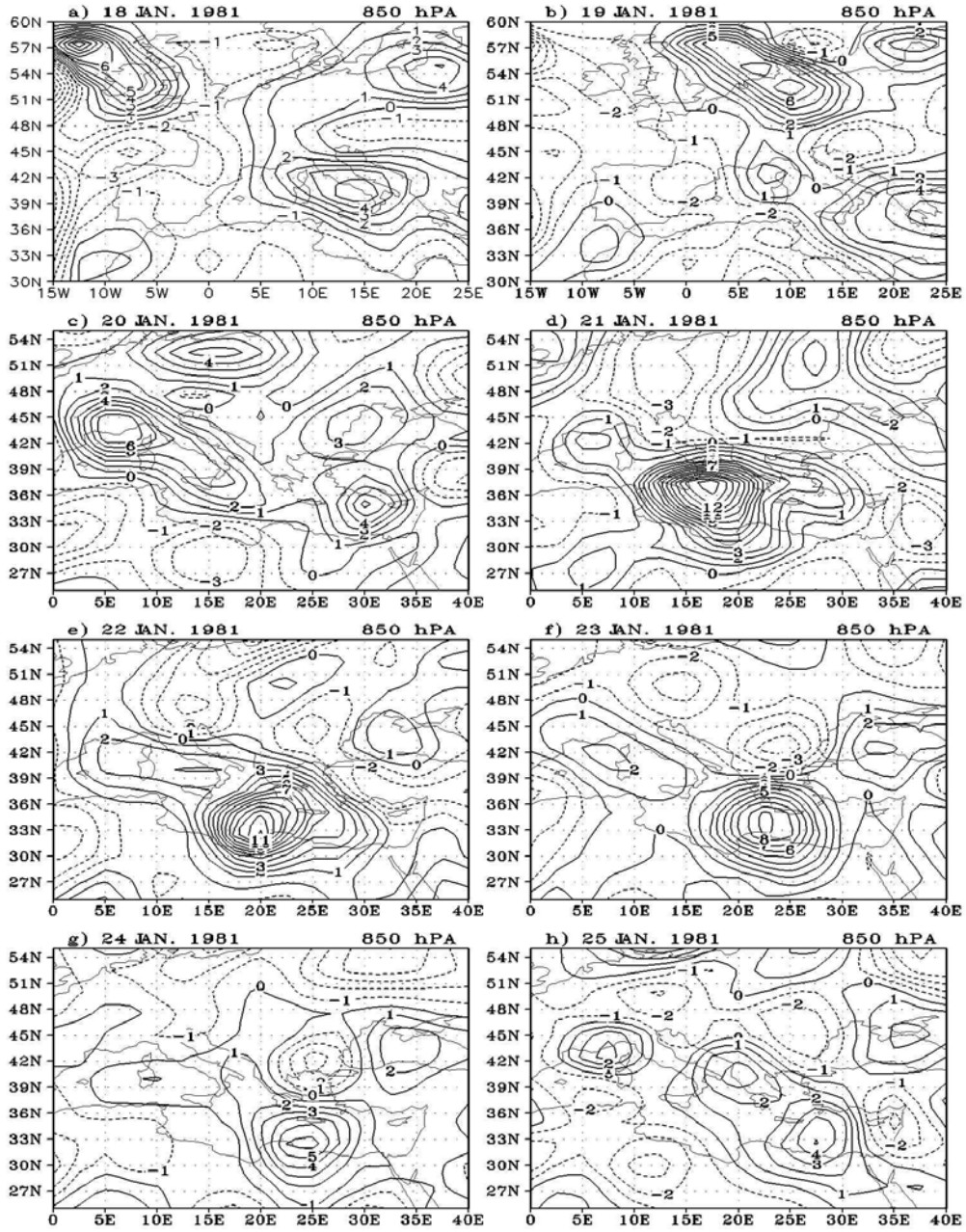

Fig. 7. Relative vorticity analysis at 850 hPa, contours every 1.0×1.0^{-4} S^{-1}, solid lines denote positive values dashed lines denote negative values for 1200 UTC 18-25 January 1981.

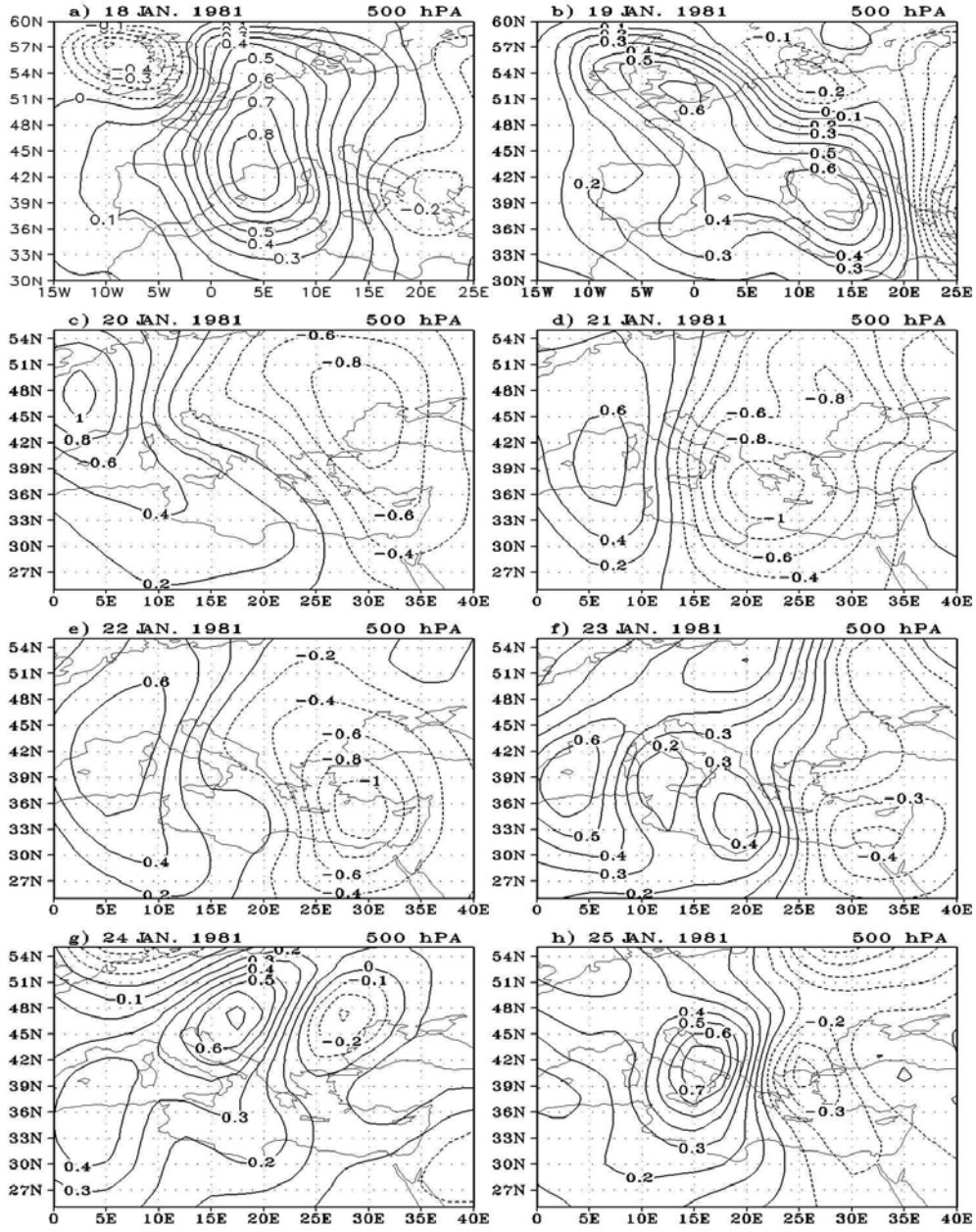

Fig. 8. Vertical motion analysis at 500 hPa contours every 0.1 Pa S^{-1}, solid lines denote positive values dashed lines denote negative values for 1200 UTC 18-25 January 1981.

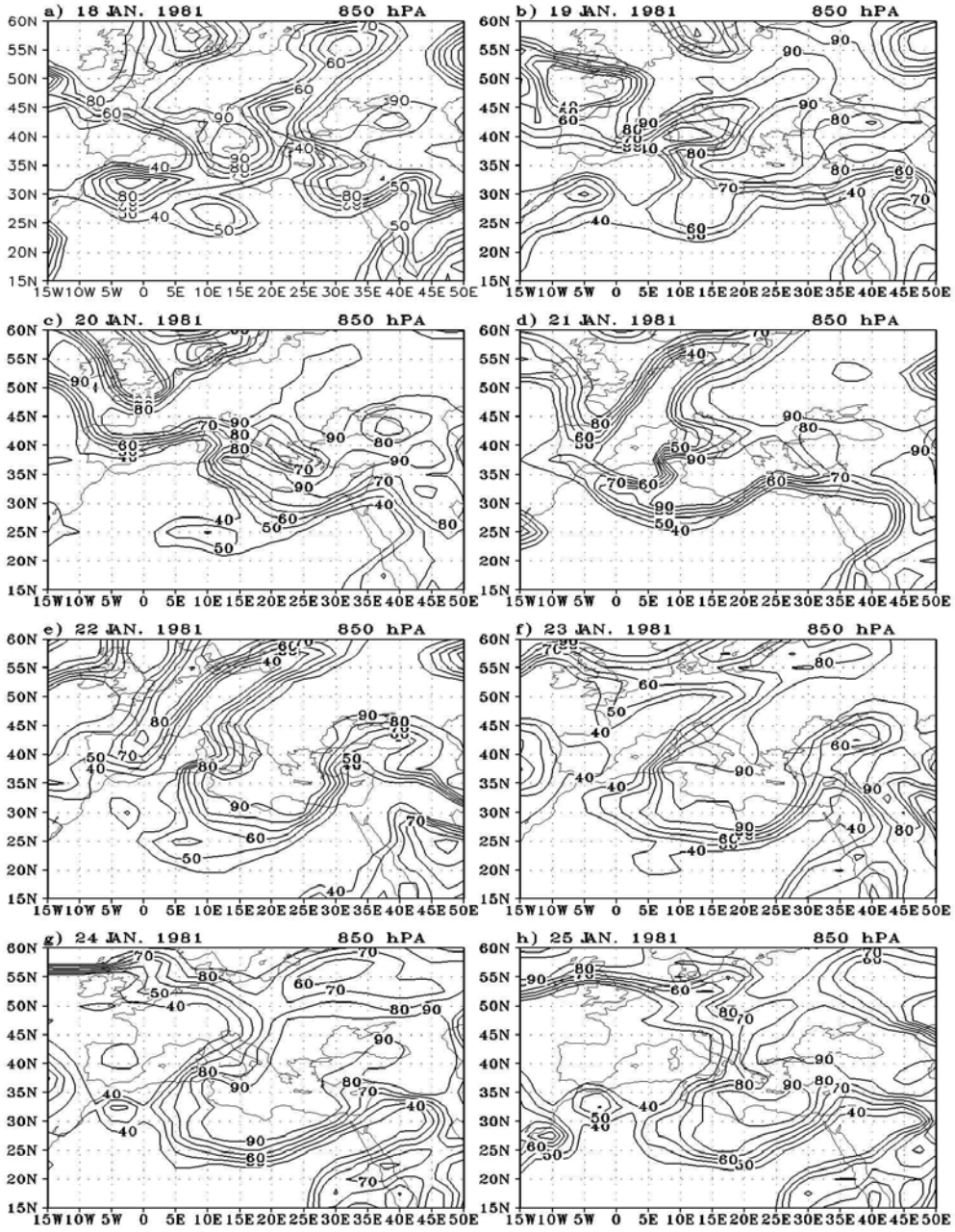

Fig. 9. Relative humidity objective analysis at 850 hPa, that ≥ 40% isopleths every 10% for 1200 UTC 18-25 January 1981.

southwards. The important feature in Figure 10b is that the PV trough extended southwards up to north Italy in the northeast-southwest direction. The larger scale dynamics is controlled by the presence of the polar jet stream on the western flank of the trough associated with intense PV gradients. On 20 January (Fig. 10c), the main core of the PV trough located over north Italy, coinciding with the 500 hPa low-pressure center, which actually developed at the same time scale. That day the PV trough extended in the northwest-southeast direction, coinciding with the 500 hPa trough. An area of low PV values appeared ahead of the PV trough over north Egypt. By 21 January the PV trough propagated southeastwards involving advection on its southern edge. The intensification of the winds resulted from the steepening of the PV gradients ahead of the trough, while the PV anomaly had reached the maximum value of 5 PVU (Fig. 10d). Also, it can be seen that the PV trough became more meridionally oriented at its southern edge.

By 22 January the trough had extended horizontally and moved slowly eastwards. The PV gradients at its southern edge have decreased significantly and two PV maximum appeared. The first was located over eastern Europe and the second was associated with high values of relative humidity (75% at 300 hPa). The first one is associated with low values of RH (< 25%, not shown), this is because the area containing the second maximum coincides with the area of ascending motion (1 Pa s^{-1} at 500 hPa), while the area of the first maximum coincides with the area of descending motion (0.6 Pa s^{-1}). That day (22 January) represents the maximum propagation of the polar front jet stream southward and also the maximum connection with the subtropical jet.

By 23 January the PV trough extended latitudinally and the associated two maximums moved southwards. The values of the first one decreased while the values of the second one increased to 4 PVU. As can be seen from Figure 2f the low became a stationary vortex rotating above the north east of the Mediterranean. Also, the two coupling maximum of PV rotating with each other.

5.2 Low-level development

The maximum deepening of the surface low pressure center at 21/12 is marked by a significant increase in the baroclinity. In particular, the potential temperature analysis at 1000 hPa (not shown) at 21/12 depicts a pronounced distortion with a thermal trough over the central Mediterranean.

It is worth noting that the wind pattern at low levels indicates a rapid intensification of the northwesterlies over the north and the central part of the Mediterranean, starting at 20/12, coincident with the deepening of the surface low pressure center. These strong surface winds became as high as 25 m/s at 21/12 (not shown) and contributed to strengthen the cold air advection which resulted in the steepening of the temperature gradients. The northwesterlies dominated over the north and central Mediterranean 24 h.

Figure 11 presents the PV analysis at 850 hPa for the period from 18 to 25 January. It displays an anomaly of magnitude 1.3 PVU located northwest of England, this anomaly is associated with values of relative humidity greater than 90%. It should be noted that this anomaly is the signature of the PV trough at 850 hPa and is connected to stratospheric air. This was verified by examining in time each of the anomalies in relation to the PV trough. According to Figure11b, within 24 h the PV maximum propagated slightly southeastwards and it became located over northeast of England.

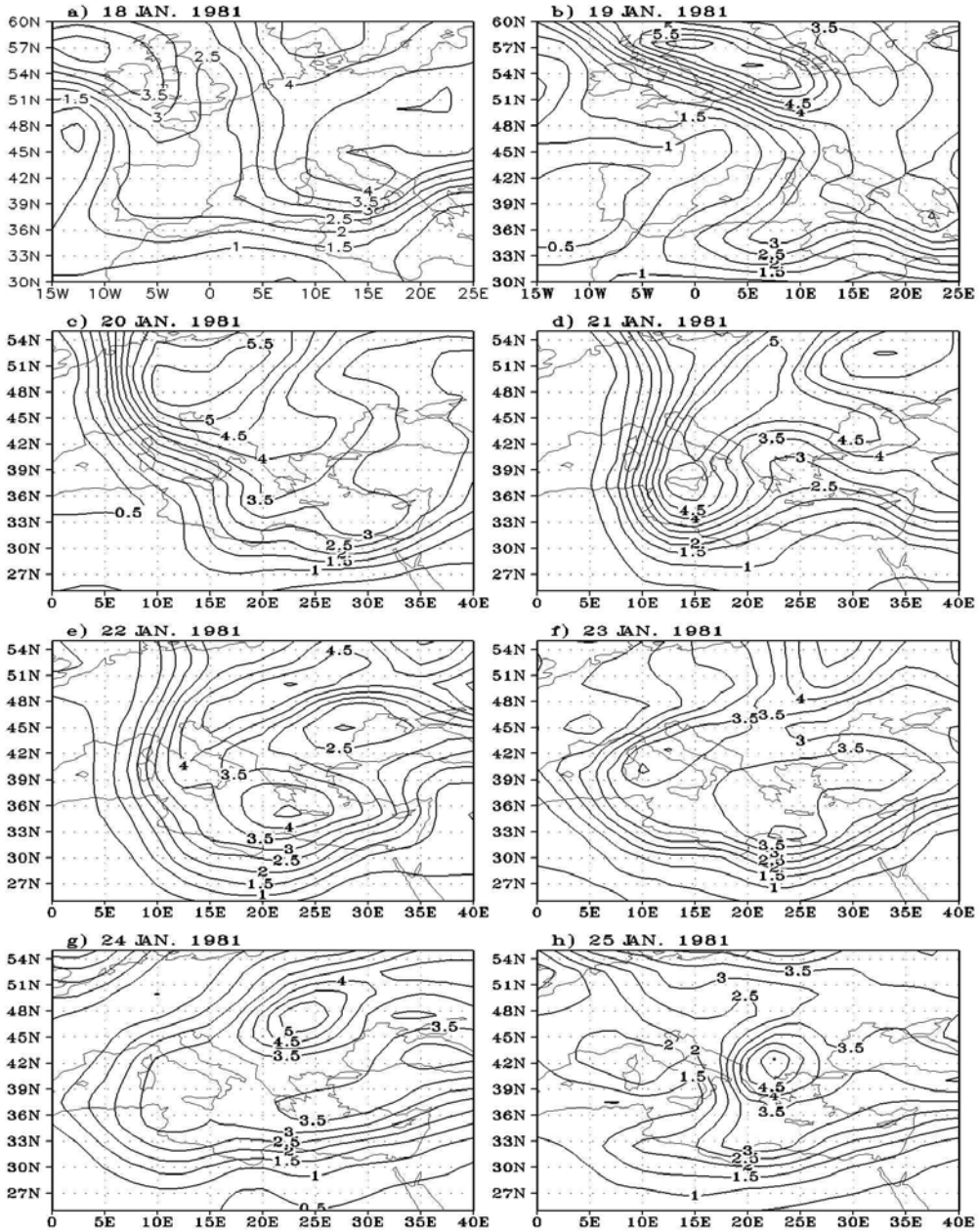

Fig. 10. Ertel´s potential vorticity on 320 K surface, contours every 0.5 PVU for 1200 UTC 18-25 January 1981. 1 PVU = 10^{-6} m^2 K kg^{-1} s^{-1}.

By 20 January (Fig. 11c) when the low-level wind pattern refer to a rapid intensification of the northerly and northwesterlies prior to the surface development, the low-level PV anomaly had propagated further to the south.

By 21 January (Fig. 11d), as the dynamic support from the upper levels decreased the low levels played the important role. The anomaly located at 42° N, 5° E on 20 January moved very fast to the southeast while the northern anomaly (45° N, 25° E) laid nearly northeast of this location. These two anomalies were joined to a quite intense low level anomaly over central Mediterranean and Romania. Just on the eastern flank of the upper level anomaly (Fig. 10d) this was accompanied by a further increase of northeasterlies of 25 m/s (not shown). It is noteworthy that the low-level PV anomaly was situated almost under the area of the tropopause warm anomaly. According to Figure 11e, within 24 h the PV maximum propagated southerly to reach the north coast of Libya and its value intensified to reach 1 PVU. At 23/12 where the system indicated cut off at all the isobaric levels, there was also a cut off of the PV anomaly and its values decreased to reach 0.8 PVU while it moved to reach the northwest coast of Egypt. It decreased generally to reach its minimum values (0.6 PVU) with the end of the period (25 January) at the north of Egypt. The period characterized by the area of PV anomalies was associated with values of relative humidity greater than 90%.

6. Summary and conclusions

The dynamics of a case of cyclogenesis over the central and northern Mediterranean, that occurred on 18-25 January 1981, have been investigated in terms of two meteorological parameters: the isobaric absolute and relative vorticity and the isentropic potential vorticity.

On the whole, the two approaches seem to identify the same features for surface cyclogenesis initiation in this case: the interaction of a region of positive absolute vorticity advection ahead of a 500 hPa trough with a shallow frontal system in the first approach, and an isentropic PV anomaly at the upper levels with a low-level baroclinic zone (that is, again with a shallow frontal system) in the second approach.

It is evident that both analyses imply the significance of the upper level dynamics in the initiation of this case of cyclogenesis. On one hand, the isobaric vorticity analysis appears to be an informative, accurate and easy method to use for describing the upper-level dynamics. On the other hand the PV analysis provided a summarized picture of the development and the evolution at upper and lower levels, which is directly visible, on the basis of a smaller number of plots compared with the isobaric vorticity analysis. The display of the time sequence of the PV on the appropriate isentropic surface helped in easily understanding the dynamics of the three-dimensional upper level development.

The PV analysis identified possible effects at low levels in the central Mediterranean (where the positive lower PV anomaly resulted from the condensation of water vapor), an area where the diabatic processes appear to play an important role in cyclonic development. Nevertheless, this point requires further investigation to determine if any of the above factors contribute to surface cyclogenesis, besides vorticity and warm advection, of course.

Therefore, the PV analysis is recommended as a more convenient and comprehensive method

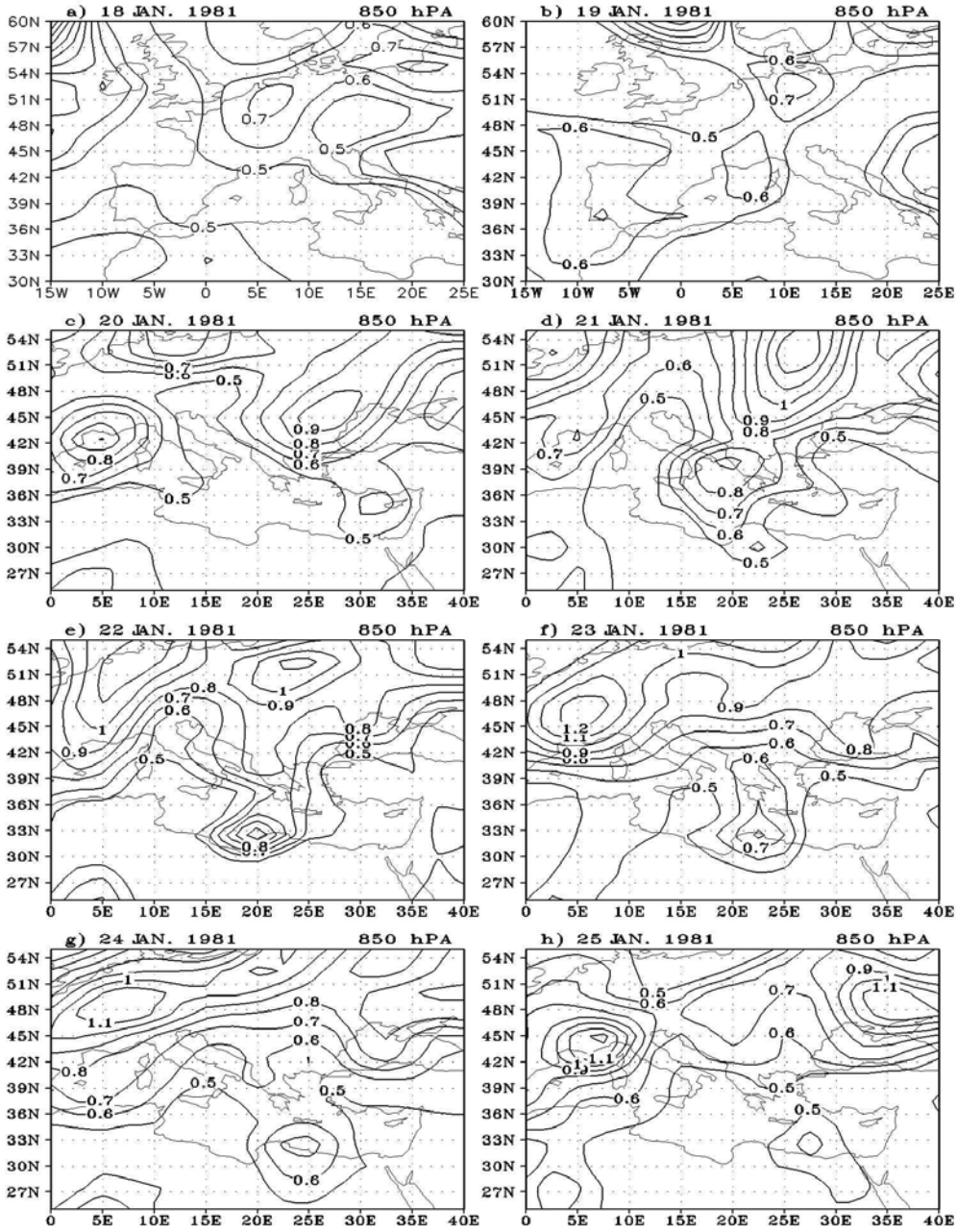

Fig. 11. Ertel´s positive potential vorticity analysis at 850 hPa, ≥ 0.5 PVU, contours every 0.1 PVU for 1200 UTC 18-25 January 1981.

for the interpretation of the dynamical mechanisms responsible for cyclogenesis over the central and northern Mediterranean region, in relation to its particular characteristics due to the geographical location and topography of the Mediterranean basin.

Another feature that invites comment is the approach of the polar front and the subtropical jets over the central Mediterranean, resulting in the amplification of the upper-level winds, the deepening of the trough and the strengthening of the vorticity maximum over the central and eastern Mediterranean. Karein (1979), following Defant (1959), believes that this interaction can play a major role in the central and eastern Mediterranean cyclogenesis during cold seasons.

References

Carlson T. S., 1991. *Mid-latitude weather systems*. Harper Collins Academic, New York, 507 p.

Defant F., 1959. On the hydrodynamic instability caused by approach of subtropical and polar front jet stream in northern latitudes before the onset of strong cyclogenesis. In: *Rossby Memorial Volume: The atmosphere and sea in motion.* B. Bolin (Ed.), Rockefeller Inst. New York, p. 305-325.

Ertel H., 1942. Ein neuer hydrodynamischer Wirbelsatz. *Meteor. Z.* **59**, 277-281.

Flocas H. A. and T. S. Karacostas, 1996. Cyclogenesis over the Aegean sea: Identification and synoptic categories. *Meteorol. Appl.* **33**, 53-61.

Holton J. R. 1979: *An introduction to dynamic meteorology*. Academic Press, New York, 391 p.

Hoskins B. J., M. E. McIntyre and A. W. Robertson, 1985. On the use and significance of isentropic potential vorticity maps. *Q. J. Roy. Meteor. Soc.* **111**, 877-946.

Karacostas T. S. and A. A. Flocas, 1983. The development of the Bomb over the Mediterranean area. *La Meteorologie* **34**, 351-358.

Karein A. D., 1979. The forecasting of cyclogenesis in the Mediterranean region. Ph.D. Thesis, University of Edinburgh, Scotland, 159 p.

Krishnamurti T. N. and L. Bounoua, 1996. *An introduction to numerical weather prediction techniques.* Academic Press, p. 73-76.

Kurz M., 1994. The role of diagnostic tools in modern weather forecasting. *Meteorol. Appl*. **1**, 45-67.

Palmen E. and C. Newton, 1969. *Atmospheric circulation systems*: *Their structure and physical interpretation.* New York and London, Academic Press, 603 p.

Petterssen S., 1956. *Weather analysis and forecasting.* Vol. 1, McGraw-Hill Book Company, 2nd. Ed. New York, 428 p.

Prezerakos N. G., 1991. Formation of sub-synoptic-scale waves on the eastern flank of a large cicyclone at 500 hPa leading to surface cyclogenesis in the Greek area on 5 October 1989. Report on the fourth session of the steering group on Mediterranean cyclones study project. WMO/TD No. 420. p. 99-110.

Prezerakos N. G., 1992. Some appreciable tropospheric circulation features leading to surface cyclogenesis in the central Mediterranean region. Extended Abstracts of Papers ICS/ICTP/

WMO International Workshop on Mediterranean Cyclones Studies, International Center for Theoretical Physics, Trieste, Italy, 18022 May, p. 74-80.

Prezerakos N. G., A. H. Flocas and S. C. Michaelides, 1999. Upper–tropospheric downstream development leading to surface cyclogenesis in the central Mediterranean. *Meteorol. Appl*. **6**, 313-322.

Rossby C. G., 1940. Planetary flow patterns in the atmosphere. *Q. J. Roy. Meteor. Soc*. **66**, 68-87.

Sanders F. and J. K. Gyakum, 1980. Synoptic-dynamic climatology of the Bombs. *Mon. Weather Rev.* **108,** 1589-1606.

Wiin-Nielsen A., 1973. *Dynamic meteorology*. WMO-No. 364, Geneva, 367 p.

WMO, 1986. Atmospheric ozone, Vol. I. Report No. 16. Geneva: WMO, 264 p.